Int. J. Solids Structures Vol. 24, No. 2, pp. 195–210, 1988
Printed in Great Britain.

0020–7683/88 $3.00+ .00

NON-LINEAR VIBRATION AND POSTBUCKLING OF UNSYMMETRIC CROSS-PLY CIRCULAR CYLINDRICAL SHELLS

V. P. Iu and C. Y. Chia
Department of Civil Engineering, University of Calgary, Calgary, Alberta, Canada T2N 1N4

(*Received* 28 *January* 1987; *in revised form* 17 *July* 1987)

Abstract—Based on von Kármán–Donnell kinematic assumptions for laminated shells, the non-linear vibration and postbuckling behaviour of unsymmetrically laminated cross-ply circular cylindrical shells with clamped and simply-supported ends are studied by a multi-mode approach. A solution is formulated and satisfies the associated compatibility equation and all boundary conditions. The transverse equation of motion is fulfilled by the Galerkin procedure. In the case of non-linear vibration problems, the solution is obtained by the method of harmonic balance. The effect of initial imperfection is also included. Results in non-linear vibration and postbuckling are presented for different amplitudes of initial imperfection and four sets of boundary conditions. Present results are compared with available data.

INTRODUCTION

Analysis of shell structures composed of composite materials has been of considerable research interest. Early work has been reviewed in a monograph by Leissa[1] and more recent literature by Bert[2]. Research has been directed to various static and dynamic analysis, as well as non-linear behaviour including postbuckling and non-linear vibrations, However, very few of the literature are concerned with the large amplitude vibration of composite shells.

The linear dynamic and static analyses of composite cylindrical shells have been conducted by many researchers using different shell theories. Based on Donnell-type theory[3], Dong[4] studied the free vibration of laminated orthotropic cylindrical shells and developed a procedure to determine the natural frequency under an arbitrary set of homogeneous boundary conditions while Bert *et al.*[5] adopted a refined Love-type theory to investigate the same problem. Other contributions in this area are attributed to Stavsky and Loewy[6], Jones and Morgan[7], Hirano[8], Greenberg and Stavsky[9], Sadasiva Rao[10], Bhimaraddi[11], Sheinman and Grief[12], and Soldatos and Tzivanidis[13]. The postbuckling behaviour of laminated cylindrical shells subject to axial load and torsion was rigorously studied by Simitses and co-workers[14–17] based on von Kármán–Donnell non-linear equations. Khot[18] studied the effects of fibre orientation and geometrical imperfection on the buckling and postbuckling behaviour. In the context of non-linear vibration, Chu[19] presented a solution for isotropic cylindrical shells while Nowinski[20] considered orthotropic cylindrical shells. Both of them concluded a hardening nonlinearity for the free flexural vibration of cylindrical shells. However, the conclusion was contradicted by the theoretical works of Evensen[21], Mayers and Wrenn[22], Evensen and Fulton[23] and the experimental work of Olson[24]. They found that a softening type of nonlinearity is possible in addition to the hardening type. Dowell and Ventres[25] derived a set of modal equations for the non-linear flexural vibrations of cylindrical shells. However, no solution was presented for these equations. A rigorous study of non-linear free flexural vibrations of circular cylindrical shells was conducted by Atluri[26] who compared his results with available data and discussed the discrepancies. He also concluded the possibility of the softening nonlinearity. El-Zaouk and Dym[27] employed the same approximation for the transverse displacement, assumed by Evensen and Fulton[23] in the analysis of isotropic cylinders, to study orthotropic doubly curved shells. However, the boundary condition of zero bending moment was violated by the assumed approximation for the transverse

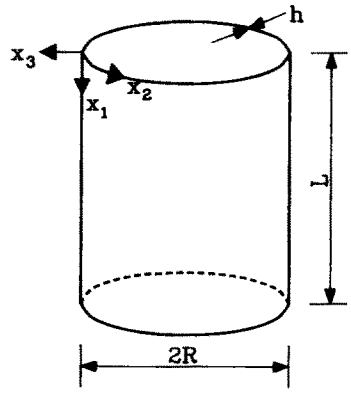

Fig. 1. Geometry and coordinate system of a circular cylindrical shell.

displacement. Recently, a finite element analysis of geometrically non-linear transient response of laminated anisotropic shells was presented by Chao and Reddy[28].

In view of the shortage of literature on the non-linear vibration of laminated cylindrical shells, the present study is directed specifically to the non-linear flexural free vibrations and postbuckling of unsymmetrically laminated cross-ply circular cylindrical shells. Based on von Kármán–Donnell kinematical assumptions, the governing equations of motion for these laminated shells are presented in the form of a compatibility equation and a transverse equation of motion. Then, a multi-mode approach is adopted to solve these equations. The solution satisfies exactly the associated boundary conditions and the compatibility equation while the transverse equation of motion is fulfilled in the approximate sense of Galerkin, leading to a set of non-linear ordinary differential equations governing the temporal description of the spatial modes assumed for the transverse displacement. Finally, these equations for time functions are solved by the method of harmonic balance. Different boundary conditions and geometrical initial imperfections are also considered. The postbuckling behaviour of laminated circular cylindrical shells is treated as a special case.

GOVERNING EQUATIONS

A circular cylindrical shell depicted in Fig. 1 is considered. Based on von Kármán–Donnell non-linear kinematic relations due to large transverse displacement and linearly elastic material behaviour, the strain–displacement relations and constitutive equations can be established. The strain–displacement relations are

$$\varepsilon_i = \varepsilon_i^0 - x_3\kappa_i \quad i = 1,2,6 \tag{1}$$

where ε_i^0 and κ_i are in-plane strains at the midsurface and bending curvatures, respectively, defined as

$$\begin{aligned}
\varepsilon_1^0 &= u_{0,1} + \tfrac{1}{2}(w_{0,1})^2 + w_{0,1}\bar{w}_{,1} \\
\varepsilon_2^0 &= v_{0,2} + w_0/R + \tfrac{1}{2}(w_{0,2})^2 + w_{0,2}\bar{w}_{,2} \\
\varepsilon_6^0 &= u_{0,2} + v_{0,1} + w_{0,1}w_{0,2} + w_{0,1}\bar{w}_{,2} + w_{0,2}\bar{w}_{,1} \\
\kappa_1 &= -w_{0,11} \quad \kappa_2 = -w_{0,22} \quad \kappa_6 = -2w_{0,12}
\end{aligned} \tag{2}$$

and the constitutive equations are

$$\begin{Bmatrix} \{\varepsilon^0\} \\ \{M\} \end{Bmatrix} = \begin{bmatrix} [A^*] & [B^*] \\ -[B^*]^{\mathrm{T}} & [D^*] \end{bmatrix} \begin{Bmatrix} \{N\} \\ \{\kappa\} \end{Bmatrix} \tag{3}$$

where

$$\{\varepsilon^0\} = [\varepsilon_1^0 \ \varepsilon_2^0 \ \varepsilon_6^0]^T$$
$$\{\kappa\} = [\kappa_1 \ \kappa_2 \ \kappa_6]^T$$
$$\{N\} = [N_1 \ N_2 \ N_6]^T$$
$$\{M\} = [M_1 \ M_2 \ M_6]^T. \tag{4}$$

In these equations, u_0, v_0, w_0 are the midsurface displacements in the x_1, x_2, x_3 directions; $\bar{w}$ is the initial transverse displacement (imperfection); N_1, N_2, N_6 are the membrane stress resultants; and M_1, M_2, M_6 are the bending moments. $[A^*]$, $[B^*]$ and $[D^*]$ are reduced stiffness matrices. Details of these matrices can be found in Ref. [29].

By the dynamic statement of the principle of virtual work and use of stress function ϕ defined as

$$N_1 = \phi_{,22}, \quad N_2 = \phi_{,11}, \quad N_6 = -\phi_{,12} \tag{5}$$

the governing equations for the non-linear flexural vibration, in particular, of unsymmetrically laminated cross-ply circular cylindrical shells may be written in the following dimensionless form of the compatibility equation:

$$L_1(F) = L_2(W) + f(W) \tag{6}$$

and transverse equation of motion

$$W_{,\tau\tau} + L_3(W) + L_2(F) + g(F, W) = Q \tag{7}$$

where

$$\begin{aligned}
L_1 &= \bar{A}_{22}^*(\ )_{,\zeta\zeta\zeta\zeta} + 2\lambda^2(\bar{A}_{12}^* + \tfrac{1}{2}\bar{A}_{66}^*)(\ )_{,\zeta\zeta\eta\eta} + \lambda^4\bar{A}_{11}^*(\ )_{\eta\eta\eta\eta} \\
L_2 &= \bar{B}_{21}^*(\ )_{,\zeta\zeta\zeta\zeta} + \lambda^2(\bar{B}_{11}^* + \bar{B}_{22}^*)(\ )_{,\zeta\zeta\eta\eta} \\
&\quad + \lambda^4\bar{B}_{12}^*(\ )_{,\eta\eta\eta\eta} + \beta(\ )_{,\zeta\zeta} + \lambda^2[2\bar{W}_{,\zeta\eta}(\ )_{,\zeta\eta} - \bar{W}_{,\eta\eta}(\ )_{,\zeta\zeta} - \bar{W}_{,\zeta\zeta}(\ )_{,\eta\eta}] \\
L_3 &= \bar{D}_{11}^*(\ )_{,\zeta\zeta\zeta\zeta} + 2\lambda^2(\bar{D}_{12}^* + 2\bar{D}_{66}^*)(\ )_{,\zeta\zeta\eta\eta} + \lambda^4\bar{D}_{22}^*(\ )_{,\eta\eta\eta\eta} \\
f(W) &= \lambda^2(W_{,\zeta\eta}^2 - W_{,\zeta\zeta}W_{,\eta\eta}) \\
g(F, W) &= \lambda^2(2F_{,\zeta\eta}W_{,\zeta\eta} - F_{,\eta\eta}W_{,\zeta\zeta} - F_{,\zeta\zeta}W_{,\eta\eta}).
\end{aligned} \tag{8}$$

The above dimensionless parameters are defined as

$$\zeta = x_1/L, \quad \eta = x_2/l, \quad l = 2\pi R/N, \quad \lambda = L/l, \quad \beta = L^2/Rh, \quad W = w_0/h, \quad \bar{w} = \bar{w}/h$$

$$F = \phi/(A_{22}h^2), \quad Q = qL^4/(A_{22}h^3), \quad \tau = \frac{t}{L^2}\sqrt{\left(\frac{A_{22}h^2}{\rho}\right)}$$

$$\bar{A}_{ij}^* = A_{22}A_{ij}^*, \quad \bar{B}_{ij}^* = B_{ij}^*/h, \quad \bar{D}_{ij}^* = D_{ij}^*/(A_{22}h^2) \quad \text{for} \quad i,j = 1,2,6 \tag{9}$$

in which N is the number of waves along the circumference, q is the transverse load, ρ is the shell mass per unit area, and t is the time. The reduction of eqns (6) and (7) to Donnell equations is obvious if the stiffness constants $\bar{A}_{ij}^*$, $\bar{D}_{ij}^*$ and $\bar{B}_{ij}^*$ are replaced by those of a singly layered isotropic material for which $\bar{B}_{ij}^*$ vanishes.

In addition to eqns (6) and (7), the cross-ply cylindrical shell is subjected to boundary conditions at the ends. In the present investigation, only four types of end conditions are considered. They are designated according to Simitses *et al.*[17] as SS1, SS3, CC1 and CC3

$$\begin{aligned}
&\text{SS1}: \quad w_0 = 0, \quad M_1 = 0, \quad N_1 = N_1^*, \quad N_6 = 0\\
&\text{SS3}: \quad w_0 = 0, \quad M_1 = 0, \quad N_1 = N_1^*, \quad v_0 = \text{const}\\
&\text{CC1}: \quad w_0 = 0, \quad w_{0,1} = 0, \quad N_1 = N_1^*, \quad N_6 = 0\\
&\text{CC3}: \quad w_0 = 0, \quad w_{0,1} = 0, \quad N_1 = N_1^*, \quad v_0 = \text{const} \quad \text{at } \zeta = 0, 1
\end{aligned} \tag{10a}$$

where N_1^* is the applied axial stress resultant at the ends. Noting eqns (2) and (3), the condition $v_0 = \text{const}$ implies

$$A_{21}^* N_1 + A_{22}^* N_2 - B_{21}^* w_{0,11} - B_{22}^* w_{0,22} = w_0/R + \tfrac{1}{2}(w_{0,2})^2 + w_{0,2}\bar{w}_{,2}. \tag{10b}$$

Then, the boundary conditions described by eqns (10) can be simplified and written in terms of the dimensionless parameters W and F as

$$\begin{aligned}
&\text{SS1}: \quad w = 0, \quad w_{,\zeta\zeta} = \lambda_1 \bar{N}_1 + \lambda_2 F_{,\zeta\zeta}, \quad \lambda^2 F_{,\eta\eta} = \bar{N}_1, \quad F_{,\zeta\eta} = 0\\
&\text{SS3}: \quad w = 0, \quad w_{,\zeta\zeta} = \lambda_3 \bar{N}_1, \quad \lambda^2 F_{,\eta\eta} = \bar{N}_1, \quad F_{,\zeta\zeta} = \lambda_4 \bar{N}_1\\
&\text{CC1}: \quad w = 0, \quad w_{,\zeta} = 0, \quad \lambda^2 F_{,\eta\eta} = \bar{N}_1, \quad F_{,\zeta\eta} = 0\\
&\text{CC3}: \quad W = 0, \quad W_{,\zeta} = 0, \quad \lambda^2 F_{,\eta\eta} = \bar{N}_1, \quad F_{\zeta\zeta} = \lambda_5 W_{,\zeta\zeta} + \lambda_6 \bar{N}_1 \quad \text{at } \zeta = 0, 1
\end{aligned} \tag{11}$$

where

$$\begin{aligned}
&\lambda_1 = -\bar{B}_{11}^*/\bar{D}_{11}^*, \quad \lambda_2 = -\bar{B}_{21}^*/\bar{D}_{11}^*\\
&\lambda_3 = (-\bar{B}_{11}^* + \bar{B}_{21}^* \bar{A}_{21}^*/\bar{A}_{22}^*)/(\bar{D}_{11}^* + \bar{B}_{21}^* \bar{B}_{21}^*/\bar{A}_{22}^*)\\
&\lambda_4 = -(\bar{A}_{21}^* + \bar{B}_{21}^* \bar{B}_{11}^*/\bar{D}_{11}^*)/(\bar{A}_{22}^* + \bar{B}_{21}^* \bar{B}_{21}^*/\bar{D}_{11}^*)\\
&\lambda_5 = \bar{B}_{21}^*/\bar{A}_{22}^*, \quad \lambda_6 = -\bar{A}_{21}^*/\bar{A}_{22}^*\\
&\bar{N}_1 = N_1^* L^2/(A_{22} h^2).
\end{aligned} \tag{12}$$

SOLUTION PROCEDURE

In view of the form of the compatibility equation and boundary conditions, the following expressions for W, $\bar{W}$ and F are assumed in the separable form as:

$$W = \sum_p \sum_q W_{pq}(\tau) X_p(\zeta) \cos 2q\pi\eta \tag{13}$$

$$\bar{W} = \sum_p \sum_q \bar{W}_{pq} X_p(\zeta) \cos 2q\pi\eta \tag{14}$$

$$F = \sum_n F_n(\zeta, \tau) \cos 2n\pi\eta + \tfrac{1}{2}\bar{N}_1 \eta^2/\lambda^2 \tag{15}$$

where

$$X_p(\zeta) = \cos p\pi\zeta - \cos (p+2)\pi\zeta \quad \text{for CC1 and CC3} \tag{16}$$

and

$$X_p(\zeta) = \sin p\pi\zeta \quad \text{for SS1 and SS3.} \tag{17}$$

Since F is to be determined through substitution of the expression for W and $\bar{W}$ into the compatibility equation, the range of index n will depend on the range of index q. It is evident that the expressions for W and $\bar{W}$ satisfy the relevant periodicity condition in the

circumferential direction together with the transverse boundary conditions except for the zero moment condition for the cases of boundary types SS1 and SS3. However, this condition is fulfilled by use of the procedure suggested by Green[30]. The essence of this procedure, in the present case, is to assume that

$$W_{,\zeta\zeta\zeta} = \sum_p \sum_q A_{pq}(\tau) \cos p\pi\zeta \cos 2q\pi\eta \tag{18}$$

and then determine $A_{pq}(\tau)$ in terms of $W_{pq}(\tau)$ by partial integration and by using the values of $W_{,\zeta\zeta}$ at ζ and 0, 1. Details of this procedure can also be found in Ref. [29].

Substituting the foregoing solution into compatibility eqn (6) and rearranging the right- and left-hand sides of the resulting eqn (6) can be written as a cosine series in η. By equating like cosine terms in η, the following set of equations is obtained:

$$\bar{A}^*_{22}F_{n,\zeta\zeta\zeta\zeta} - 2\lambda^2(2n\pi)^2(\bar{A}^*_{12} + \tfrac{1}{2}\bar{A}^*_{66})F_{n,\zeta\zeta} + \lambda^4(2n\pi)^4\bar{A}^*_{11}F_n$$

$$= \sum_m [g_{1mn}(\tau) \sin m\pi\zeta + f_{1mn}(\tau) \cos m\pi\zeta] \quad \text{for SS1 and SS3} \tag{19}$$

$$= \sum_m [g_{1mn}(\tau) + f_{1mn}(\tau)] \cos m\pi\zeta \quad \text{for CC1 and CC3} \tag{20}$$

where the range of index m is related to the range of index p by

$$g_{1mn}(\tau) = \sum_p \sum_q g^{pq}_{1mn} W_{pq}(\tau)$$

$$f_{1mn}(\tau) = \sum_p \sum_q \sum_r \sum_s [g^{pqrs}_{2mn} W_{pq}(\tau)\bar{W}_{rs} + g^{pqrs}_{3mn} W_{pq}(\tau) W_{rs}(\tau)]. \tag{21}$$

The constants g^{pq}_{1mn}, g^{pqrs}_{2mn} and g^{pqrs}_{3mn} are presented in the Appendix.

The complete solution F_n to eqn (19) can obviously be written as the sum of the complementary function and a particular solution

$$F_n(\zeta, \tau) = F^c_n(\zeta, \tau) + F^p_n(\zeta, \tau). \tag{22}$$

Simply by inspection, the particular solution F^p_n can readily be shown to be

$$F^p_n(\zeta, \tau) = \sum_m [\bar{g}_{1mn}(\tau) \sin m\pi\zeta + \bar{g}_{2mn}(\tau) \cos m\pi\zeta + \bar{g}_{3mn} \cos m\pi\zeta] \quad \text{for SS1 and SS3} \tag{23}$$

$$= \sum_m [\bar{g}_{1mn}(\tau) + \bar{g}_{2mn}(\tau) + \bar{g}_{3mn}(\tau)] \cos m\pi\zeta \quad \text{for CC1 and CC3} \tag{24}$$

where

$$\bar{g}_{imn}(\tau) = g_{imn}(\tau)/b_{mn} \quad \text{for } i = 1, 2, 3$$

$$b_{mn} = (m\pi)^4\bar{A}^*_{22} + 2\lambda^2(2n\pi)^2(m\pi)^2(\bar{A}^*_{12} + \tfrac{1}{2}\bar{A}^*_{66}) + \lambda^4(2m\pi)^4\bar{A}^*_{22}. \tag{25}$$

On the other hand, the complementary solution F^c_n to the homogeneous form of eqn (19) can be shown without difficulty to have the form

$$n = 0, \quad F_0^c(\zeta, \tau) = \sum_{k=1}^{4} a_{0k}(\tau)\zeta^{k-1} \tag{26}$$

$$n \neq 0, \quad F_n^c(\zeta, \tau) = \sum_{k=1}^{4} a_{nk}(\tau)\, e^{\gamma_{nk}\zeta} \tag{27}$$

where γ_{nk}'s are roots of the characteristic equation

$$\bar{A}_{22}^* \gamma^4 - 2\lambda^2(2n\pi)^2(\bar{A}_{22}^* + \tfrac{1}{2}\bar{A}_{66}^*)\gamma^2 + \lambda^4(2n\pi)^4 \bar{A}_{11}^* = 0 \tag{28}$$

the roots of which all possess real values for cross-ply laminates composed of graphite–epoxy, glass–epoxy and boron–epoxy materials. The unknown parameters $a_{nk}(\tau)$ in eqns (26) and (27) are to be determined. Substitution of eqn (15) into in-plane boundary conditions yield the following conditions for F_n.

$$\begin{aligned}
&\text{SS1 and CC1:} \quad && F_n = 0, \quad F_{n,\zeta} = 0 \\
&\text{SS3:} && F_n = 0, \quad F_{0,\zeta\zeta} = \lambda_4 \bar{N}_1, \quad F_{n,\zeta\zeta} = 0 \\
&\text{CC3:} && F_n = 0, \quad F_{0,\zeta\zeta} = \lambda_5 \sum_p W_{p0}(\tau) X_p''(\zeta) + \lambda_6 \bar{N}_1 \\
& && F_{n,\zeta\zeta} = \lambda_\zeta \sum_p W_{pn}(\tau) X_p''(\zeta) \quad \text{at } \zeta = 0, 1.
\end{aligned} \tag{29}$$

Inserting expression (22) for F_n into these boundary conditions and expressing all terms involving the unknown a_{nk} in terms of all other terms, a set of four equations for each n is furnished and written in a general form as

$$[E_n]\{a_n\} = \{y_n\} \tag{30}$$

where $[E_n]$ is a matrix with constant elements and $\{y_n\}$ is a vector with elements as linear functions of $\bar{N}_1$, $\sum_p \sum_q W_{pq}(\tau)$, $\sum_p \sum_q \sum_r \sum_s W_{pq}(\tau)\bar{W}_{rs}$ and $\sum_p \sum_q \sum_r \sum_s W_{pq}(\tau) W_{rs}(\tau)$ and where $\{a_n\} = [a_{n1}(\tau), a_{n2}(\tau), a_{n3}(\tau), a_{n4}(\tau)]^T$. Hence, the a_{nk}'s are determined by solving eqn (30) with the result

$$a_{nk}(\tau) = C_{0nk}\bar{N}_1 + \sum_p \sum_q C_{1nk}^{pq} W_{pq}(\tau) + \sum_p \sum_q \sum_r \sum_s C_{2nk}^{pqrs} W_{pq}(\tau)\bar{W}_{rs} + \sum_p \sum_q \sum_r \sum_s C_{3nk}^{pqrs} W_{pq}(\tau) W_{rs}(\tau) \tag{31}$$

in which C_{0nk}, C_{1nk}^{pq}, C_{2nk}^{pqrs} and C_{3nk}^{pqrs} are constant coefficients but are not presented here in full. However, they can be computed systematically. So far, the expressions for W and F satisfying both the compatibility equation and boundary conditions are obtained. In order to derive time equations for $W_{pq}(\tau)$ by eliminating the spatial dependence from the transverse equation of motion, the Galerkin procedure is applied to eqn (7) which leads to the following conditions:

$$\int_0^1 \int_0^1 [W_{,\tau\tau} + L_3(W) + L_2(F) + g(F, W) - Q] X_i(\zeta) \cos 2j\pi\eta \, d\zeta \, d\eta = 0 \quad i, j = 1, 2, 3, \ldots \tag{32}$$

Utilizing eqns (13)–(15), (22)–(24), (26), (27) and (31), and performing the above integration, a set of non-linear ordinary differential equations for $W_{pq}(\tau)$ is furnished

$$\alpha_{ij}^{pq} W_{pq}(\tau)_{,\tau\tau} + (\beta_{ij}^{pq} + \bar{N}_1 \bar{\beta}_{ij}^{pq}) W_{pq}(\tau) + \gamma_{ij}^{pqrs} W_{pq}(\tau) W_{rs}(\tau) + \mu_{ij}^{pqrstu} W_{pq}(\tau) W_{rs}(\tau) W_{tu}(\tau) = Q_{ij} - \bar{N}_1 (\bar{\beta}_{ij}^{pq} \bar{W}_{pq} + \xi_{ij}) \quad (33)$$

where α_{ij}^{pq}, β_{ij}^{pq}, $\bar{\beta}_{ij}^{pq}$, γ_{ij}^{pqrs}, μ_{ij}^{pqrstu}, and ξ_{ij} are constants where

$$Q_{ij} = \int_0^1 \int_0^1 Q X_i(\zeta) \cos 2j\pi\eta \, d\zeta \, d\eta. \quad (34)$$

The foregoing set of equations with quadratic and cubic nonlinearities forms the basic system for the subsequent non-linear vibration analysis of cross-ply cylindrical shells by the method of harmonic balance. Each time function $W_{pq}(\tau)$ is expanded into a Fourier cosine series

$$W_{pq}(\tau) = \sum_{k=0}^{\infty} W_k^{pq} \cos k\omega\tau \quad (35)$$

which is sufficient for undamped periodic vibrations and in which ω is dimensionless vibrating frequency and W_k^{pq} the unknown coefficient on the kth harmonic amplitude. The dimensionless vibrating frequency ω is related to the vibrating frequency $\bar{\omega}$ by

$$\omega = \bar{\omega} L^2 \sqrt{\left(\frac{\rho}{A_{22} h^2}\right)}. \quad (36)$$

The implementation of the method of harmonic balance to solve eqn (33) is a tedious and laborious task but can be handled systematically by a computer for an arbitrary number of terms in the Fourier cosine expansion. A simple algorithm in association with a routine for solving non-linear algebraic equations has been developed to serve this purpose. By neglecting the time dependence, eqn (33) reduces to a set of non-linear algebraic equations ready for the postbuckling analysis.

NUMERICAL RESULTS AND DISCUSSIONS

A number of examples in non-linear vibration and postbuckling are presented for unsymmetrically laminated cross-ply circular cylindrical shells composed of graphite–epoxy material. The elastic constants typical of this used in calculations are

$$E_L/E_T = 40, \quad G_{LT}/E_T = 0.5, \quad \nu_{LT} = 0.25$$

where E_L and E_T are the principal moduli of elasticity of an orthotropic material, G_{LT} is the shear modulus and ν_{LT} is Poisson's ratio. Numerical results are computed by using three asymmetric and three axisymmetric modes in the circumferential direction while the first six terms are considered in the Fourier series expansion (35). Because of the quadratic and cubic types of nonlinearity of eqn (33), the significance of the harmonic amplitudes corresponding to $\cos 4\omega\tau$ and $\cos 5\omega\tau$ has numerically demonstrated to be negligibly small.

For completeness, the numerical procedure for obtaining the amplitude–frequency responses by solving eqn (33) is briefly described. With the implementation of the harmonic balance method, eqn (33) is simplified to a set of non-linear algebraic equations for the harmonic amplitudes W_k^{pq} and the dimensionless non-linear frequency ω if $\bar{N}_1$ is zero. However, the number of non-linear algebraic equations is equal to the product of the number of equations in eqn (33) and the number of terms in the Fourier cosine expansion for each $W_{pq}(\tau)$. By prescribing one of the unknowns among W_k^{pq} and ω, the resulting non-linear algebraic equations can readily be solved by any standard routine for non-linear equations provided that a good initial guess is given. By successively solving these non-linear equations with a prescribed unknown and an initial approximation, the amplitude–frequency response can be traced. The prescribed unknown is chosen as one of the harmonic

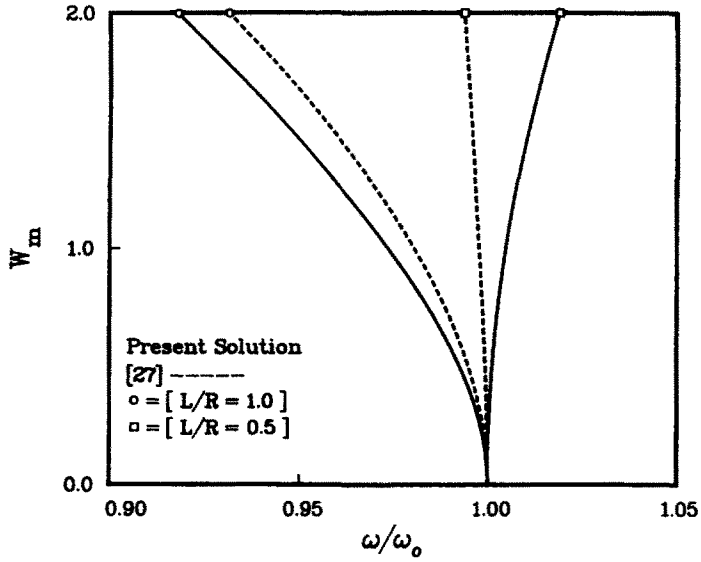

Fig. 2. Comparison of non-linear frequencies of glass–epoxy orthotropic circular cylindrical shells with SS3 boundary condition ($R/h = 100$, $N = 5$, $E_L/E_T = 3$, $G_{LT}/E_T = 0.5$, $\nu_{LT} = 0.25$).

amplitudes and ω which has shown the greatest change in the last solution step while the initial guess is approximated by the previous solution or an extrapolation from several of the calculated solutions. Usually, the prescribed value is one of the harmonic amplitudes as they change faster than ω, especially when the amplitude of vibration is small. However, the difference of the prescribed unknown and the corresponding unknown in the previous solution should be kept small to ensure proper convergence. Once a solution in terms of harmonic amplitude and frequency ω is computed, the maximum amplitude W_m at the mid-section can then be determined from a plot of the dimensionless transverse displacement W at $\zeta = 0.5$ vs the dimensionless time τ over a period of 2π. Actually, the location of the maximum amplitude on the τ-axis can be easily pinpointed by inspection because the first few harmonic amplitudes usually bear the greater contributions than the higher ones.

The results are presented in tables and graphs in association with the dimensionless compressive load $-\bar{N}_1$, frequency ratio ω/ω_0 where ω_0 is the dimensionless linear frequency similarly defined as in eqn (36) and the dimensionless W_m which is the maximum magnitude of the dimensionless transverse displacement W at the mid-section of the cylinder. It is worthy to mention that no results are available in non-linear free vibrations and post-buckling of laminated cross-ply cylinders. Also, the present solution does not apply to the isotropic case for which the roots of eqn (28) are not distinct, rendering a different form of solution for the complementary F_n^c in eqn (22) though the solution procedure remains valid. Nevertheless, it is applicable to orthotropic cylindrical shells. Present results for the non-linear vibration of a simply-supported orthotropic cylindrical shell composed of glass–epoxy material are compared in Fig. 2 with those given by El-Zaouk and Dym[27]. It is noted that the solution of El-Zaouk and Dym does not satisfy the zero bending moment condition at the ends of the cylinder, especially when the amplitude of vibration grows larger, and restrains the participation of the axisymmetric deformation while the present solution satisfies all boundary conditions. Therefore, discrepancies between two sets of values are observed even at small amplitudes of vibration. For the case with $L/R = 0.5$ the present solution demonstrated a hardening behaviour whereas Ref. [27] shows a very weakly softening effect.

For antisymmetric cross-ply circular cylindrical shells the dimensionless linear frequencies of various cases shown in Figs 3–8 are listed in Table 1 while Table 2 contains the dimensionless buckling loads for different types of boundary conditions. Present critical values are in good agreement with exact values obtained by Dong[4] as indicated in these tables. It is noted that in all examples except for those in Fig. 5, the circumferential wave number N is associated with the fundamental modes of vibration or the lowest buckling load.

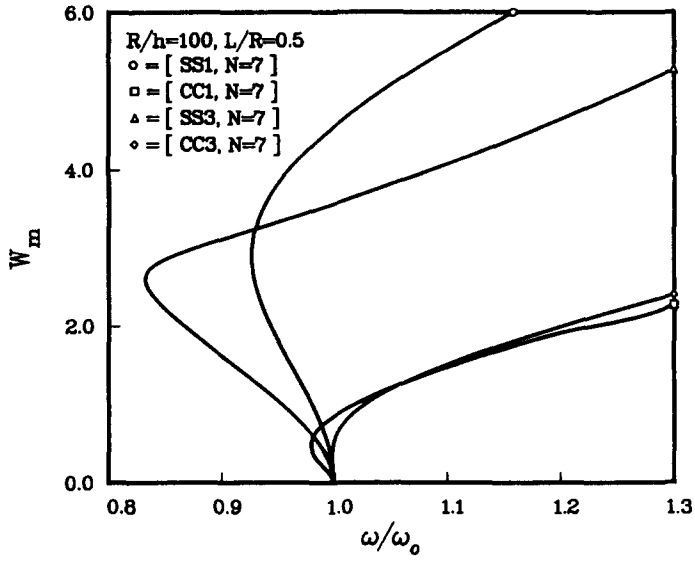

Fig. 3. Non-linear frequencies of the first mode of graphite–epoxy cross-ply [0°/90°] circular cylindrical shells with different boundary conditions.

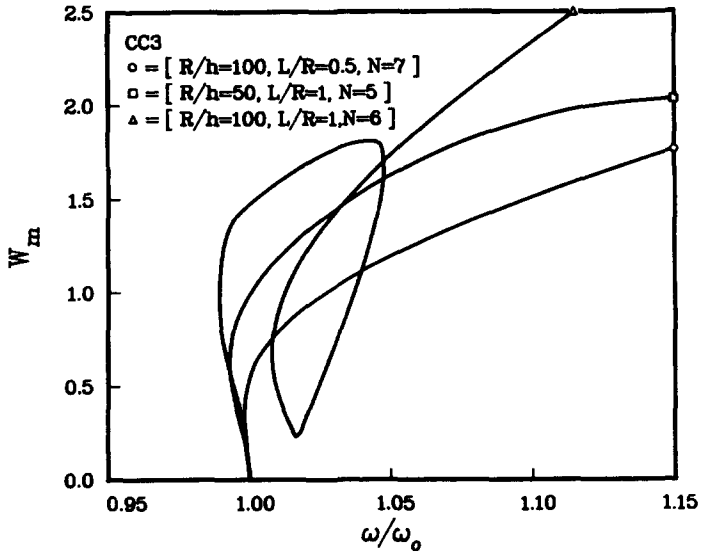

Fig. 4. Amplitude–frequency responses of graphite–epoxy cross-ply [0°/90°] circular cylindrical shells with CC3 boundary condition.

Typical amplitude–frequency responses for the four types of the aforementioned boundary conditions are demonstrated in Fig. 3 where all response curves exhibit initial softening trends and revert to hardening at large amplitudes although the degree of softening and hardening vary. This is basically similar to the findings in the non-linear vibration of isotropic cylindrical shells and orthotropic cylindrical shells as presented by Evensen[21, 23], Mayers and Wrenn[22], and El-Zaouk and Dym[27]. Not unexpectedly, the responses of clamped cylinders show much stronger nonlinearity than those of simply-supported cylinders at large amplitudes. Despite the different degrees of softening and hardening behaviours for different boundary conditions, there is a common approximately linear variation of amplitudes and frequency at large amplitude vibrations. As there are regions where the amplitude is not unique for a given frequency, jump phenomena may happen in experiments or real situations.

It is interesting to note that internal resonance is detected in the non-linear free vibration of cylindrical shells with the CC3 boundary condition as shown in Fig. 4 by the response curve corresponding to the case with $L/R = 1$, $N = 6$ and $R/h = 100$. This

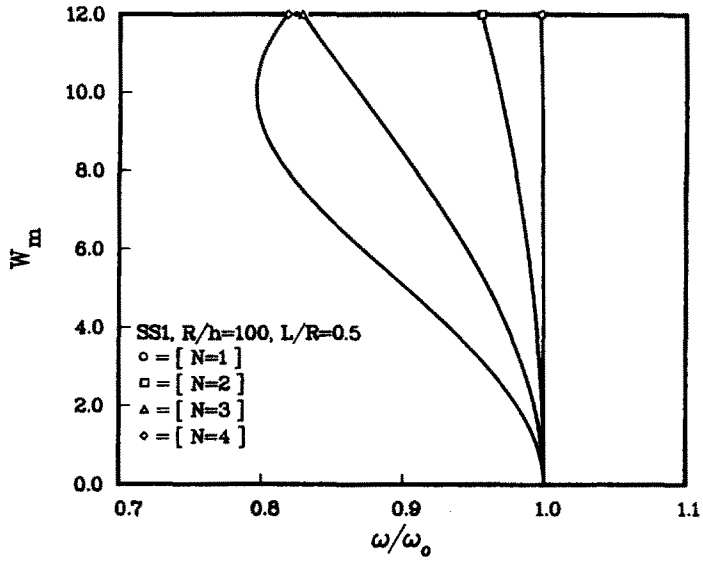

Fig. 5. Effect of circumferential wave number on amplitude–frequency responses of graphite–epoxy cross-ply [0°/90°] circular cylindrical shells with SS1 boundary condition.

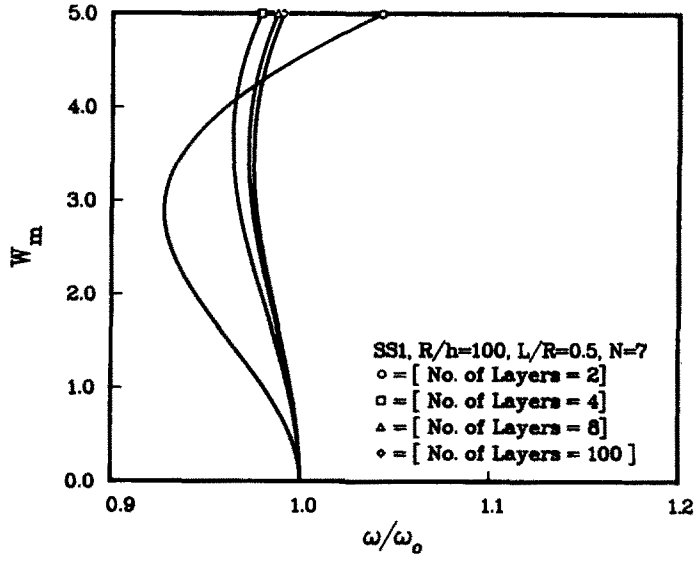

Fig. 6. Effect of number of layers on non-linear frequencies of the first mode of graphite–epoxy antisymmetric cross-ply circular cylindrical shells with SS1 boundary condition.

amplitude–frequency response presents a softening behaviour and bends towards the direction of increasing frequency, then at the frequency ratio approximately equal to 1.05 drops drastically with decreasing frequency and finally grows again with the hardening behaviour. Such a looping characteristic is due to the fact that the nonlinearity exists, the second mode of vibration the maximum amplitude of which does not occur at the mid-section. Hence, the maximum amplitude W_m decreases. In other words, the vibrating energy is transferred from the first mode to the second mode when W_m decreases and then the process reverses as W_m increases again. The phenomenon of internal resonance is possible whenever some of the natural frequencies (nonlinear) are commensurable. Details of internal resonance are described in Ref. [31]. It is because of the multi-mode approach and the method of harmonic balance with many terms in the expansion that internal resonance is found. Fewer modes and a smaller number of harmonic terms have revealed such a phenomenon.

Figure 5 shows an increase of the circumferential wave number N amplifies the softening and hardening behaviour of amplitude–frequency responses for the case of SS1 while

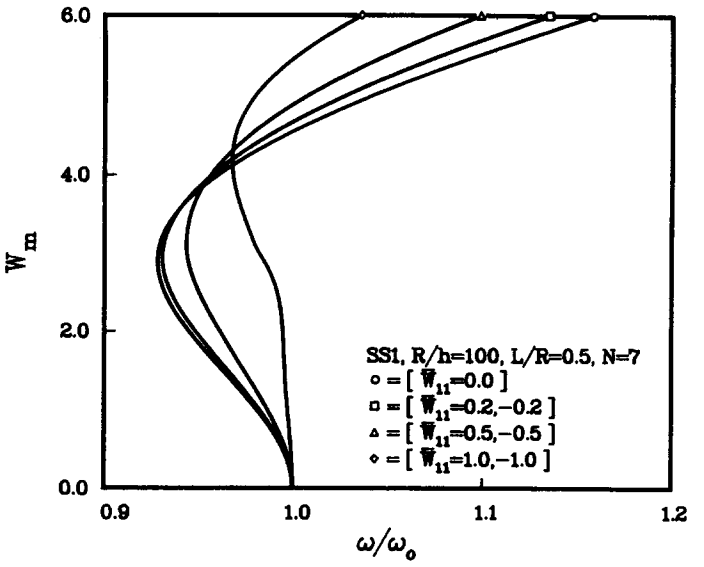

Fig. 7. Effect of asymmetric initial imperfections on non-linear frequencies of the first mode of graphite–epoxy cross-ply [0°/90°] circular cylindrical shells with SS1 boundary condition.

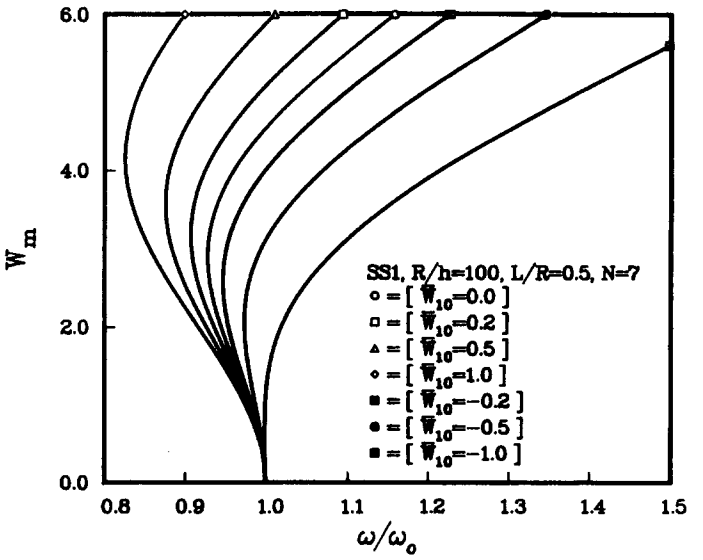

Fig. 8. Effect of axisymmetric initial imperfections on non-linear frequencies of the first mode of graphite–epoxy cross-ply [0°/90°] circular cylindrical shells with SS1 boundary condition.

an increase of the number of layers in the laminates weakens the nonlinearity as demonstrated in Fig. 6. As to study the effect of the initial imperfection which may take axisymmetric or asymmetric form, the amplitude–frequency responses of a cross-ply cylinder with an SS1 boundary condition are presented. For asymmetric imperfection with a prescribed value for $\bar{W}_{11}$ and zero values for other $\bar{W}_{pq}$ are shown in Fig. 7, the magnitudes of imperfection, either positive or negative, reduce the degree of nonlinearity. However, for axisymmetric imperfection with prescribed $\bar{W}_{10}$ and zero values for others, the amplitude–frequency responses shown in Fig. 8 are affected both by the magnitudes and the direction of the imperfection. Positive imperfections soften the overall behaviour while negative imperfections, on the contrary, demonstrate hardening effects.

Finally, examples on postbuckling behaviour with asymmetric imperfections are presented for the aforementioned four types of boundary conditions. The results are presented in Figs 9–12. For the case of $\bar{W}_{11} = 0$ or $\bar{W}_{01} = 0$ corresponding to perfect shells, the response curves depict a typical postbuckling behaviour of shells which is characterized by a decrease of the load carrying capacity and then an increase at large deflections. In other

Table 1. Comparison of dimensionless linear frequencies of graphite–epoxy antisymmetric cross-ply circular cylindrical shells used in Figs 2–7

Figure No.	Boundary condition	R/h	L/R	N	No. of layers	$\bar{W}_{10}$ or $\bar{W}_{11}$	ω_0 Present	ω_0 Dong[4]
3	SS1	100	0.5	7	2		4.1547	4.1531
	SS3	100	0.5	7	2		4.4031	4.4031
	CC1	100	0.5	7	2		5.6828	5.6654
	CC3	100	0.5	7	2		5.7084	5.6965
4	CC3	100	0.5	7	2		5.7084	5.6965
		50	1	5	2		7.7257	7.7141
		100	1	6	2		11.1255	11.0575
5	SS1	100	0.5	1	2		8.1855	8.1371
				2	2		7.1063	7.0763
				3	2		6.0150	5.9984
				4	2		5.1608	5.1517
6	SS1	100	0.5	7	2		4.1547	4.1531
				6	4		5.0829	5.0820
				6	8		5.2694	5.2684
				6	100		5.3297	5.3287
7	SS1	100	0.5	7	2	0.0	4.1547	4.1531
						0.2	4.3495	—
						0.5	4.6528	—
						1.0	5.1815	—
						−0.2	3.9670	—
						−0.5	3.7013	—
						−1.0	3.3122	—
8	SS1	100	0.5	7	2	0.0	4.1547	4.1531
						±0.2	4.1549	—
						±0.5	4.1564	—
						±1.0	4.1727	—

Table 2. Comparison of the lowest dimensionless buckling loads of graphite–epoxy cross-ply [0°/90°] circular cylindrical shells

Boundary condition	R/h	L/R	N	$\bar{N}_{cr}$ Present	$\bar{N}_{cr}$ Dong[4]
SS1	100	0.5	7	1.7386	1.7370
SS3	100	0.5	7	1.9644	1.9644
CC1	100	0.5	8	2.5754	2.5746
CC3	100	0.5	8	2.5802	2.5794

words, non-unique deformations are possible for a given axial load. When there are initial imperfections, the load–deflection curves are modified as demonstrated in these figures. It is evident that the imperfections have greater influence on the decrease of the so-called limit load for the case of SS3 than SS1, as claimed by Simitses *et al.*[17] though the difference is not as prominent as those examples of Simitses. The behaviours of the load–deflection curves for all four types of boundary conditions at large deflections reveal a similar linear deflection as pointed out for the amplitude–frequency responses in non-linear vibration. An increase in the load-carrying capacity with increasing magnitudes of imperfection is observed for all boundary conditions except for the case of CC1 where load–deflection curves with imperfection approach the perfect one asymtotically at large deflections.

In the non-linear vibration of isotropic cylinders, Evensen and Fulton[23] contradicted the results of Chu[19] who claimed only the hardening-type behaviour for amplitude–frequency responses was possible. The difference is rooted in the assumed approximations for the transverse displacement. It is clear that Evenson and others[23, 25, 26] employed approximations which are composed of both asymmetric and axisymmetric variations while

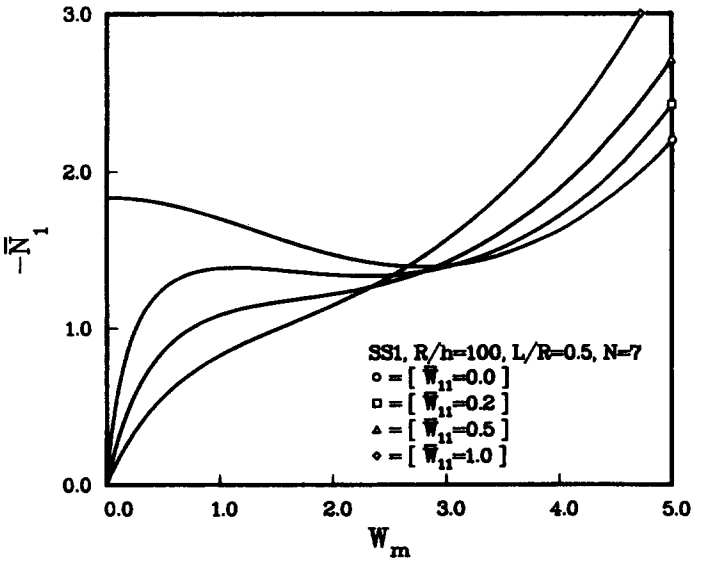

Fig. 9. Postbuckling responses of graphite–epoxy cross-ply [0°/90°] circular cylindrical shells with SS1 boundary condition and different asymmetric initial imperfections.

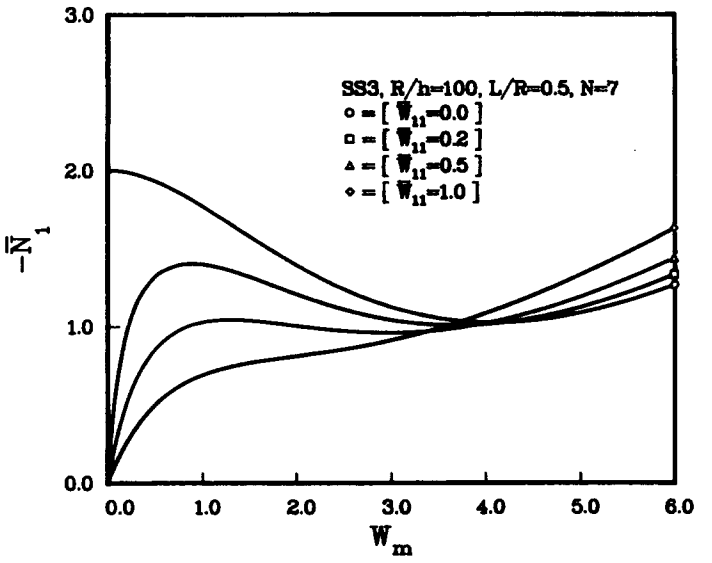

Fig. 10. Postbuckling responses of graphite–epoxy cross-ply [0°/90°] circular cylindrical shells with SS3 boundary condition and different asymmetric initial imperfections.

Chu employed only an asymmetric representation for the transverse displacement, which automatically resulted in the vanishing of quadratic nonlinearity. Such a nonlinearity is proved to produce the softening-type behaviour. In the present multi-mode analysis which enables arbitrary selection of mode shapes, both the axisymmetric and asymmetric deformations have shown their participation in non-linear vibration and postbuckling behaviour though they are uncoupled in linear analysis. Hence, the inclusion of axisymmetric deformations in the non-linear analysis of cylindrical shells is essential.

CONCLUSION

Based on von Kármán–Donnell type non-linear theory for unsymmetrically laminated cross-ply circular cylindrical shells, a multi-mode solution is formulated and applied to study the non-linear vibration as well as the postbuckling behaviour. The results shown are in agreement with those for the vibration and buckling of laminated cross-ply cylindrical shells. It is observed that in the non-linear vibration of these cylinders, the non-linear effects

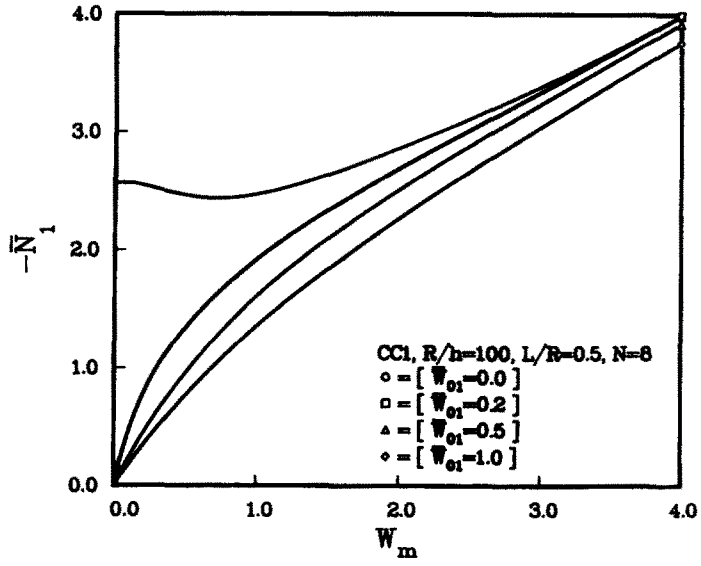

Fig. 11. Postbuckling responses of graphite–epoxy cross-ply [0°/90°] circular cylindrical shells with CC1 boundary condition and different asymmetric initial imperfections.

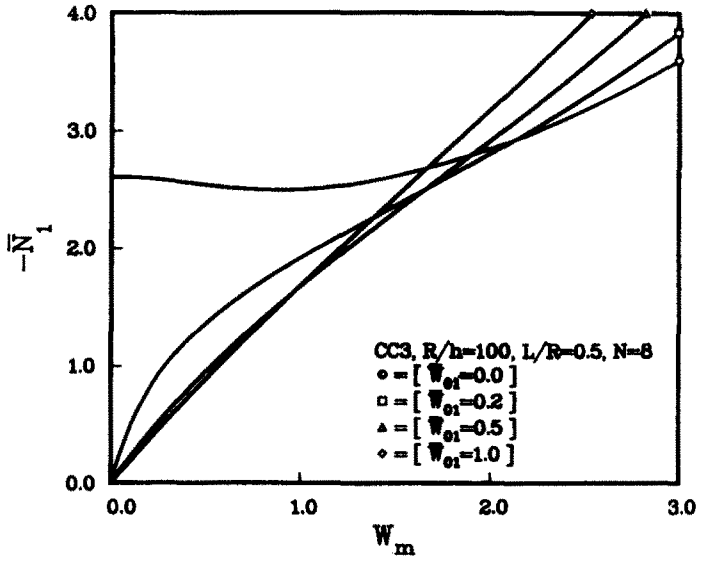

Fig. 12. Postbuckling responses of graphite–epoxy cross-ply [0°/90°] circular cylindrical shells with CC3 boundary condition and different asymmetric initial imperfections.

can be initially of the softening type and reverts to the hardening type at large amplitudes of vibration. It is evident that axisymmetric deformations are indispensable for non-linear analysis of cylindrical shells. In the case of the CC3 boundary condition, internal resonance is observed as a result of the provision of a multi-mode approach and the method of harmonic balance with an arbitrary number of harmonic terms. As the present formulation is general in nature, non-linear vibrations of cross-ply cylinder subjected to axial load and transverse load can also be studied.

Acknowledgement—The results presented in this paper were obtained in the course of research sponsored by the Natural Sciences and Engineering Research Council of Canada.

REFERENCES

1. A. W. Leissa, Vibration of shells. NASA SP-288 (1973).
2. C. W. Bert, Vibration of composite structures. *Proc. Int. Conf. on Recent Advances in Structural Dynamics*, Institute of Sound and Vibration Research, University of Southampton, pp. 693–712 (1980).

3. L. H. Donnell, Stability of thin-walled tubes under torsion. NACA Report 479 (1933).
4. S. B. Dong, Free vibration of laminated orthotropic cylindrical shells. *J. Acoust. Soc. Am.* **44,** 1628–1635 (1968).
5. C. W. Bert, J. L. Baker and D. M. Egle, Free vibration and multilayer anisotropic cylindrical shells. *J. Comp. Mater.* **3,** 480–499 (1969).
6. Y. Stavsky and R. Loewy, On vibrations of heterogeneous orthotropic cylindrical shells. *J. Sound Vibr.* **15,** 255–256 (1971).
7. R. Jones and H. Morgan, Buckling and vibration of cross-ply laminated circular cylindrical shells. *AIAA J.* **13,** 664–671 (1975).
8. Y. Hirano, Buckling of angle-ply laminated circular cylindrical shells. *J. Appl. Mech.* **46,** 233–234 (1979).
9. J. B. Greenberg and Y. Stavsky, Vibrations of laminated filament-wound cylindrical shells. *AIAA J.* **19,** 1055–1062 (1981).
10. Y. V. K. Sadasiva Rao, Vibrations of layered shells with transverse shear and rotatory inertia effects. *J. Sound Vibr.* **86**(1), 147–150 (1983).
11. A. Bhimaraddi, Dynamic response of orthotropic homogeneous and laminated cylindrical shells. *AIAA J.* **23,** 1834–1837 (1985).
12. I. Sheinman and S. Grief, Dynamic analysis of laminated shells of revolution. *J. Comp. Mater.* **18,** 200–215 (1984).
13. K. P. Soldatos and G. J. Tzivanidis, Buckling and vibration of cross-ply laminated non-circular shells. *J. Sound Vibr.* **82,** 425–434 (1982).
14. D. Shaw, G. J. Simitses and I. Sheinman, Imperfect, laminated cylindrical shells in torsion and axial compression. *Acta Mech.* **10,** 395–400 (1983).
15. I. Sheinman, D. Shaw and G. J. Simitses, Nonlinear analysis of axially-loaded laminated cylindrical shells. *Comput. Struct.* **16,** 131–137 (1983).
16. G. J. Simitses, D. Shaw, I. Sheinman and J. Giri, Imperfection sensitivity of fiber-reinforced, composite thin cylinders. *Comp. Sci. Technol.* **22,** 259–276 (1985).
17. G. J. Simitses, D. Shaw and I. Sheinman, Stability of cylindrical shells by various nonlinear shell theories. *ZAMM* **65,** 159–166 (1985).
18. N. S. Khot, Buckling and postbuckling behaviour of composite cylindrical shells under axial compression. *AIAA J.* **8,** 229–235 (1970).
19. H. N. Chu, Influence of large amplitude on flexural vibrations of a thin circular cylindrical shell. *J. Aero. Sci.* **28,** 602–609 (1961).
20. J. L. Nowinski, Nonlinear transverse vibrations of orthotropic cylindrical shells. *AIAA J.* **1,** 617–620 (1963).
21. D. A. Evensen, Some observations on the nonlinear vibration of thin cylindrical shells. *AIAA J.* **1,** 2857–2858 (1963).
22. J. Mayers and B. G. Wrenn, On the nonlinear free vibrations of thin cylindrical shells. *Dev. Mech.* **4,** 819–846 (1967).
23. D. A. Evensen and R. E. Fulton, Some studies on the nonlinear dynamic response of shell-type structures. Int. Conf. Dynamic Stab. Struct. (Edited by G. Hermann), pp. 237–254 (1965).
24. M. D. Olson, Some experimental observations on the nonlinear vibration of cylindrical shells. *AIAA J.* **3,** 1775–1777 (1965).
25. E. H. Dowell and C. S. Ventres, Modal equations for the nonlinear flexural vibrations of a cylindrical shell. *Int. J. Solids Structures* **4,** 975–991 (1968).
26. S. Atluri, A perturbation analysis of non-linear free flexural vibrations of a circular cylindrical shell. *Int. J. Solids Structures* **8,** 549–569 (1972).
27. B. R. El-Zaouk and C. L. Dym, Non-linear vibrations orthotropic doubly-curved shallow shells. *J. Sound Vibr.* **31,** 89–103 (1973).
28. W. C. Chao and J. N. Reddy, Analysis of laminated composite shells using a degenerate 3-D element. *Int. J. Numer. Meth. Engng* **20,** 1991–2007 (1984).
29. C. Y. Chia, *Nonlinear Analysis of Plates.* McGraw-Hill, New York (1980).
30. A. E. Green, Double Fourier series and boundary value problems. *Proc. Camb. Phil. Soc.* **40,** 222–228 (1944).
31. A. H. Nayfeh and D. T. Mook, *Nonlinear Oscillations.* Wiley, New York (1979).

APPENDIX

For boundary types SS1 and SS3

$$g^{pq}_{1mn} = [\bar{B}^*_{21} p^4\pi^4 + \lambda^2(\bar{B}^*_{11} + \bar{B}^*_{22}) p^2\pi^2 (2q\pi)^2 + \lambda^4 \bar{B}^*_{12} (2q\pi)^4 - \beta p^2\pi^2]\, \delta^p_m\, \delta^q_n$$

in which δ^i_j is the Kronecker delta.

For boundary types CC1 and CC3

$$\begin{aligned} g^{pq}_{1mn} = {} & \{\bar{B}^*_{21}[p^4\pi^4\delta^p_m - (p+2)^4\pi^4\delta^{p+2}_m] + \lambda^2(\bar{B}^*_{11} + \bar{B}^*_{22}) \\ & \times [p^2\pi^2\delta^p_m - (p+2)^2\pi^2\delta^{p+2}_m]\,(2q\pi)^2 + \lambda^4 \bar{B}^*_{12}(\delta^p_m - \delta^{p+2}_m)\,(2q\pi)^2 \\ & - \beta[p^2\pi^2\delta^p_m - (p+2)^2\pi^2\delta^{p+2}_m]\}\,\delta^q_n \end{aligned}$$

$$g^{pqrs}_{2mn} = 4\lambda^2[8qs\pi^2 I^{mpr}_1 J^{nqs}_1 + 4s^4\pi^2 I^{mpr}_2 J^{nqs}_2 + 4q^2\pi^2 I^{mrp}_2 J^{nqs}_2]/(1+\delta^n_0)\,(1+\delta^m_0)$$

$$g^{pqrs}_{3mn} = 4\lambda^2[4qs\pi^2 I^{mpr}_1 J^{nqs}_1 + 4s^2\pi^2 I^{mpr}_2 J^{nqs}_2]/(1+\delta^n_0)\,(1+\delta^m_0)$$

where

$$I_1^{mpr} = \int_0^1 X_p' X_r' \cos m\pi\zeta \, \mathrm{d}\zeta$$

$$I_2^{mpr} = \int_0^1 X_p'' X_r \cos m\pi\zeta \, \mathrm{d}\zeta$$

$$J_1^{nqs} = \int_0^1 \sin 2q\pi\eta \sin 2s\pi\eta \cos 2n\pi\eta \, \mathrm{d}\eta$$

$$J_2^{nqs} = \int_0^1 \cos 2q\pi\eta \cos 2s\pi\eta \cos 2n\pi\eta \, \mathrm{d}\eta.$$